AD-A119 219 SPECTRON DEVELOPMENT LABS INC COSTA MESA CA F/G 20/4
AERODYNAMIC DROPLET BREAKUP.(U)
MAY 82 J E CRAIG
UNCLASSIFIED SDL-82-2193-06 AFOSR-TR-82-0698 NL

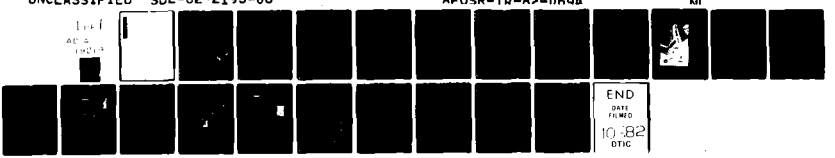

(1)

AERODYNAMIC DROPLET BREAKUP

(Annual Technical Report)

J. E. Craig

24 May 1982

SDL NO. 82-2193-06

Prepared For:

Dr. Leonard Caveny
Air Force Office
of
Scientific Research

SPECTRON
DEVELOPMENT
LABORATORIES
INC.

3303 Harbor Boulevard, Suite G-3
Costa Mesa, California 92626 (714) 549-8477

TABLE OF CONTENTS

LIST OF FIGURES

INTRODUCTION

Combustion efficiency of aluminized propellants in solid rocket motors is reduced by incomplete aluminum combustion and two-phase nozzle flow losses. The combustion of aluminized propellants can produce large Al/Al_2O_3 agglomerates. The agglomerate dynamics within the combustion chamber and nozzle have a significant influence on the overall combustion efficiency of the motor. Agglomerates are subjected to large aerodynamic loads within the rocket nozzle where the gas phase experiences a more rapid acceleration than the agglomerates. The drag load deforms the agglomerates and if of sufficient magnitude can result in breakup. The smaller fragments have faster velocity and thermal equilibrium times and have higher combustion rates. For maximum combustion efficiency the aluminum fragments must completely oxidize, achieve the exhaust gas velocity, and transfer their thermal energy to the gas phase. As a direct result of agglomerate breakup, the aluminum combustion rate is increased, and the thermal energy released is efficiently transferred into exhaust kinetic energy.

Photographic observations obtained in windowed rocket motors and combustion bombs indicate relatively large agglomerates (100μm - 500μm) are formed on the propellant surface and entrained in the combustion flow; however, particle size measurements obtained from sampling the exhaust plumes indicate small mean particle diameters (10μm). These small exhaust plume particles appear to result from the breakup of the larger agglomerates during the nozzle expansion process. Observations of agglomerate breakup in a laboratory scale rocket nozzle revealed an adequate correlation with Weber number; however, neither the physical process of breakup nor the fragment size distribution was resolved.

This research has the objective of obtaining physical data to characterize the mechanisms of aerodynamic droplet breakup. The first of a multiphase experiment has been completed in which conventional liquids (water, alcohol, glycerine, etc.) were studied. The primary goal of this initial phase was to examine the effect of liquid properties (viscosity and surface tension) on the breakup mechanism, time scale, and fragment size distribution. The future plans propose to investigate droplets formed from low melting point metals--aluminum and aluminum/aluminum oxide agglomerates.

A key element of the experimental effort is the use of pulsed laser holography to resolve the breakup of liquid droplets and agglomerates in simulated rocket nozzle flows. High resolution, large depth-of-field, a coherent light source, and short exposure times (characteristic of high energy pulsed laser holography) provide an opportunity to observe particle breakup mechanisms with a degree of detail not previously possible.

RESEARCH STATUS

Aerodynamic droplet breakup is characterized by the magnitude and duration of the aerodynamic forces. For nozzle contractions, the droplets are loaded as a result of the higher gas phase acceleration. The droplets respond to the aerodynamic forces by deforming and accelerating. The initial acceleration scales with the initial diameter; however, as the pressure forces flatten the droplet, increasing its cross-sectional area, the drag load increases rapidly. This sequence of events can, of course, lead to catastrophic deformation and droplet breakup if the slip velocity is of sufficient magnitude and duration.

The liquid surface tension is used to scale the aerodynamic load forming the Weber number;

$$We = \frac{\rho \, \Delta v^2 \, \phi_d}{\sigma_d}$$

ρ = lensity

Δv = slip velocity

ϕ = diameter

σ = surface tension

The duration of the aerodynamic loading can be scaled by the natural period for hydrodynamic oscillation,

$$\tau_n \simeq \left(\frac{\rho_d \, \phi_d^{\,3}}{\sigma_d} \right)^{1/2}$$

For nozzle accelerations, an additional time scale exists; namely the time required for velocity equilibrium, τ_v. Assuming the droplet Reynolds number relative to the gas phase is sufficienty high (i.e., $Re > 10^3$), the

drag coefficient for rigid droplets is approximately unity and the corresponding time scale is

$$\tau_v = \frac{\rho_d \phi_d}{\rho \Delta v} .$$

However, since the droplets are not rigid but elastic, the droplet cross section and the associated drag load increase rapidly within the nozzle contraction. Therefore, the time scale for liquid droplet velocity equilibrium is no doubt faster than the rigid droplet estimate.

An experiment was designed in which droplet deformations could be investigated in a nozzle contraction. The nozzle was designed to allow droplet injection upstream of the contraction. Windows formed the sides of the two-dimensional nozzle allowing observation of the droplet interaction. The gas is delivered from a settling chamber through a sintered metal throttle to the nozzle plenum where the droplets are injected. The nozzle contraction ratio is eight as the initial 12 mm x 100 mm cross section reduces to 12 mm x 12 mm at the nozzle exit. At maximum compressor capacity, the nozzle exit velocity and flowrate are 180 m/s and 20 gm/sec, respectively.

Piezoelectric droplet generators were constructed to produce highly monodisperse droplet streams. Droplet diameters were varied from 50 μm to to 1200 μm for water, glycerine/water mixtures, alcohol, and freon liquids. The droplet generation frequency varied from 100 Hz for large diameters to 10^4 Hz for small diameters. The basic design was that of modern ink jet printers. The complete droplet generator is composed of a liquid supply tank, electrical driver, and the ink-jet devices (Figure 1). The ink jets were assembled into an encasing tube which was mounted in the nozzle facility (Figure 2). For the experiments, the droplets were injected at a velocity of about 1 m/s.

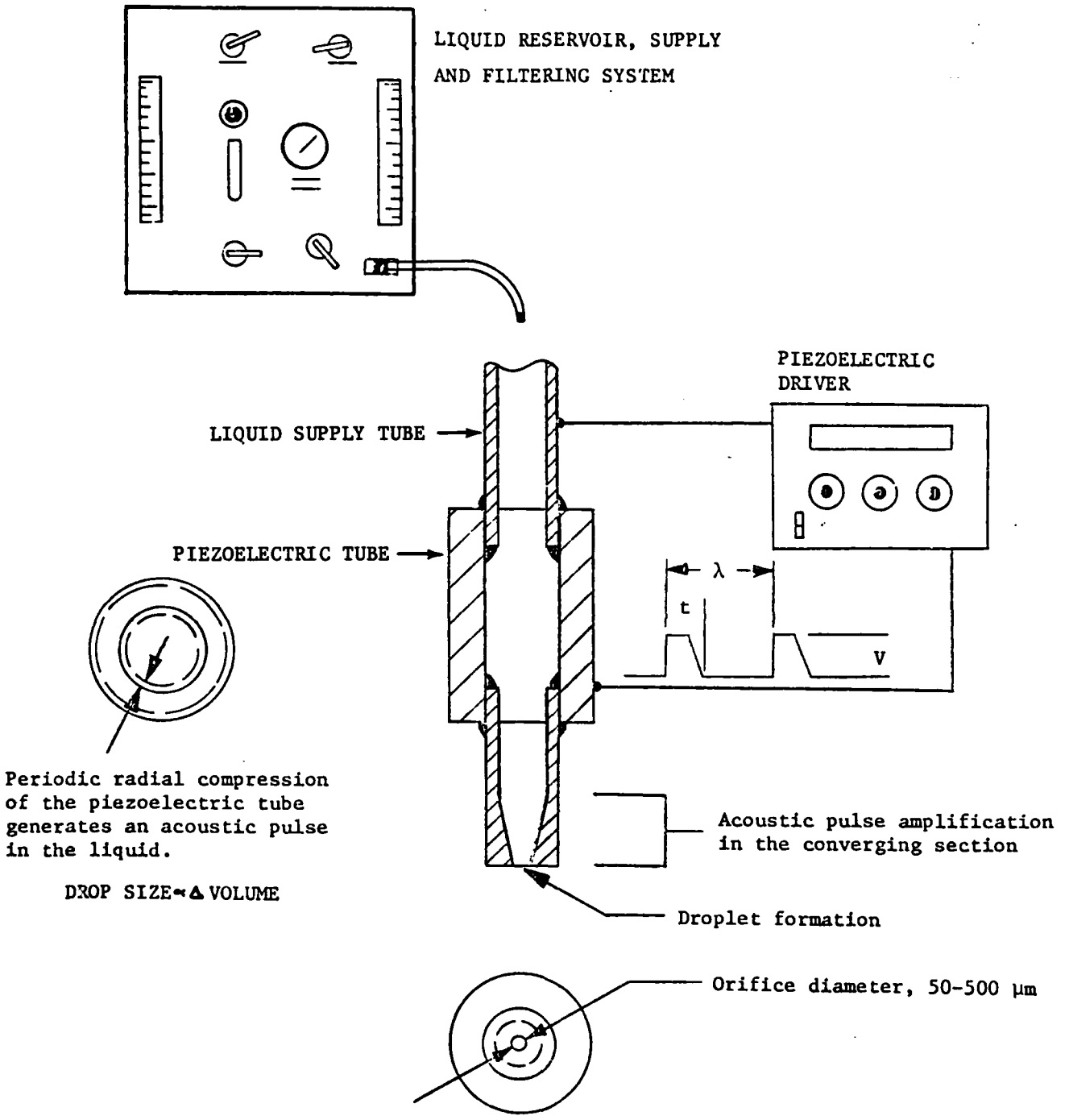

FIGURE 1. Single Element Monodisperse Generator System

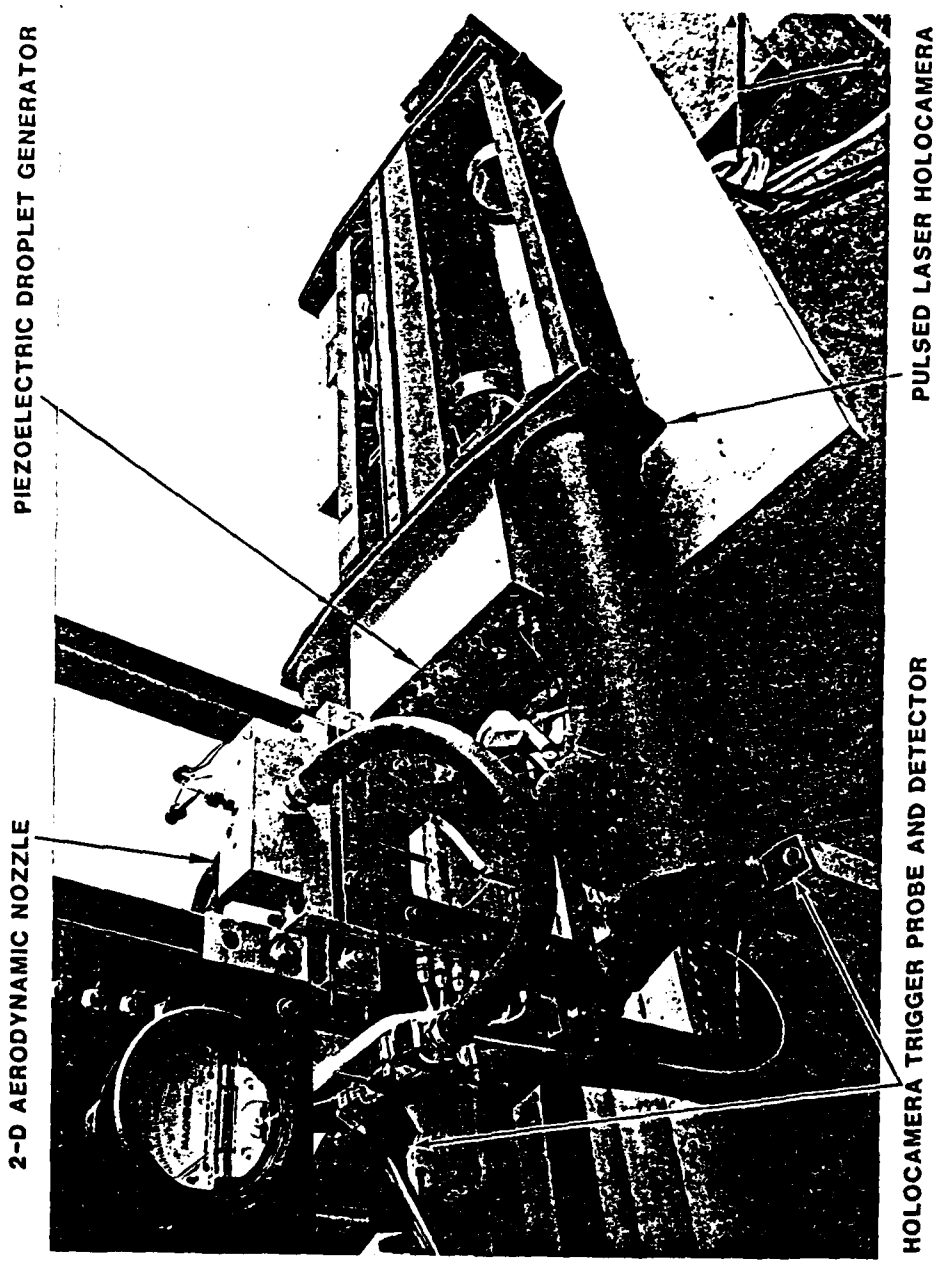

Figure 2. Aerodynamic Droplet Breakup Experiment

Holographic observation of the droplet interaction within the nozzle contraction were produced. The holocamera viewing optics were configured with object-to-hologram image magnifications of one and five. The large field-of-view optics (ϕ = 100 mm diameter, 1x magnification) were used in the initial experiments in which the droplet velocities were measured along the nozzle. Double exposure ($\Delta t \sim 10\mu s$) holography is used to observe droplet velocity. Smaller field-of-view optics (ϕ = 25 mm diameter, 5x magnification) were used to record high resolution observations of the droplet breakup process. For this case, external triggering is required to center the droplet position in the hologram. With premagnification (5x) the holocamera spatially resolves 4 μm in reconstruction. Since the holograms are recorded in 10^{-8} seconds, droplets of order 10 μm diameter can be resolved at velocities approaching 10^{3} m/s. For these experiments the droplet velocities were limited to about 100 m/s.

For each group of experiments, a data set characterizing the conditions was prepared. The droplet and gas phase velocity profiles within the nozzle contraction constitute the primary data (Figure 3). The gas velocity in the nozzle exit is estimated from local measurements of total and static pressures. The velocity profile is estimated from incompressible flow theory. The droplet velocities are determined from double-pulse holography; however, as the droplets approach breakup, the weaker portions experience higher accelerations and have higher velocities than the more massive portions. Droplet failure occurs very soon after the velocity becomes nonuniform. After failure, velocities were not measured. The slip velocity profile is calculated directly. This velocity profile is integrated to determine the elapsed time along the nozzle. With the slip velocity and the elapsed time, the Weber number

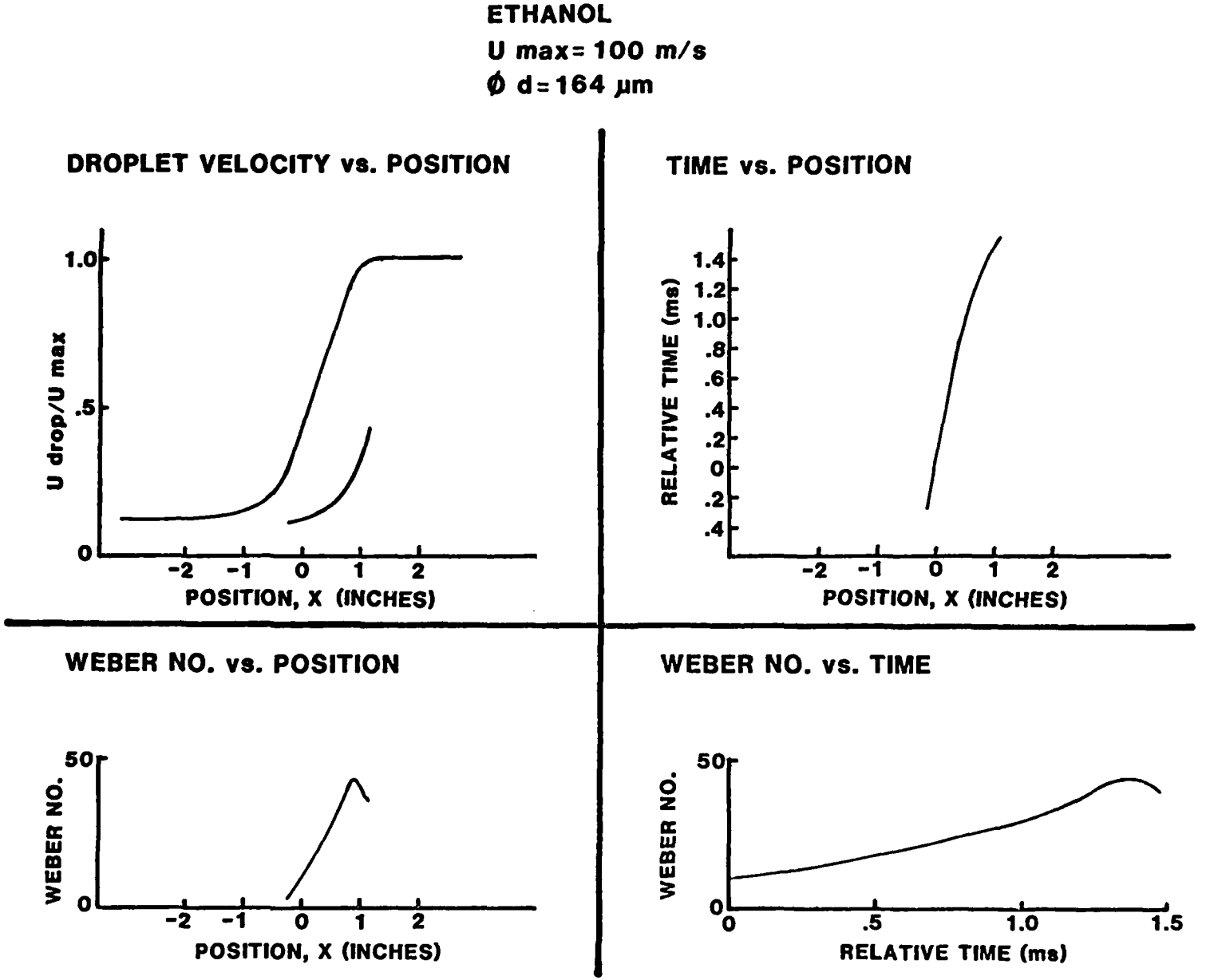

FIGURE 3. Droplet Dynamics Data Presentation (Ethanol, ϕ_o = 164 µm, ΔV_{MAX} = 100 m/s).

history is calculated based on the initial droplet diameter. The time is initialized to zero at a point within the nozzle where the Weber number becomes significant (i.e., We = 10). Hence, a well-defined loading history associated the droplet deformation and breakup process observed in the holograms is defined including peak Weber number and breakup time.

Surface Tension Variations

Two liquids, alcohol and water, were selected to examine the effects of surface tension. Droplet size and nozzle flowrates were regulated to obtain equivalent peak Weber numbers of 47 and 51, respectively. Examples of sequential stages of the droplet breakup process are displayed in Figure 4. The classical bag breakup mode is observed to occur for each liquid, indicating that the Weber number is an adequate scaling parameter. In addition, the breakup times for each liquid are about the same ($t_c \simeq 3.0$).

Initially the droplet flattens under the high pressure exerted on the stagnation point. As the droplet flattens, its radius of curvature increases and the stagnation pressure is felt over a larger area. The droplet is unstable to this form of loading. The center of the droplet is eventually pushed downstream of the outer edge forming a thin membrane in the shape of a bag. When the bag bursts, very small fragments are formed; however, considerable mass still remains in the annular ring. The annular ring fails last producing the largest fragments. Hence failure is observed in two stages; the initial stage in which deformations of sufficient magnitude are experienced that the droplet could never recover to its original shape, and the final stage in which fragmentation occurs.

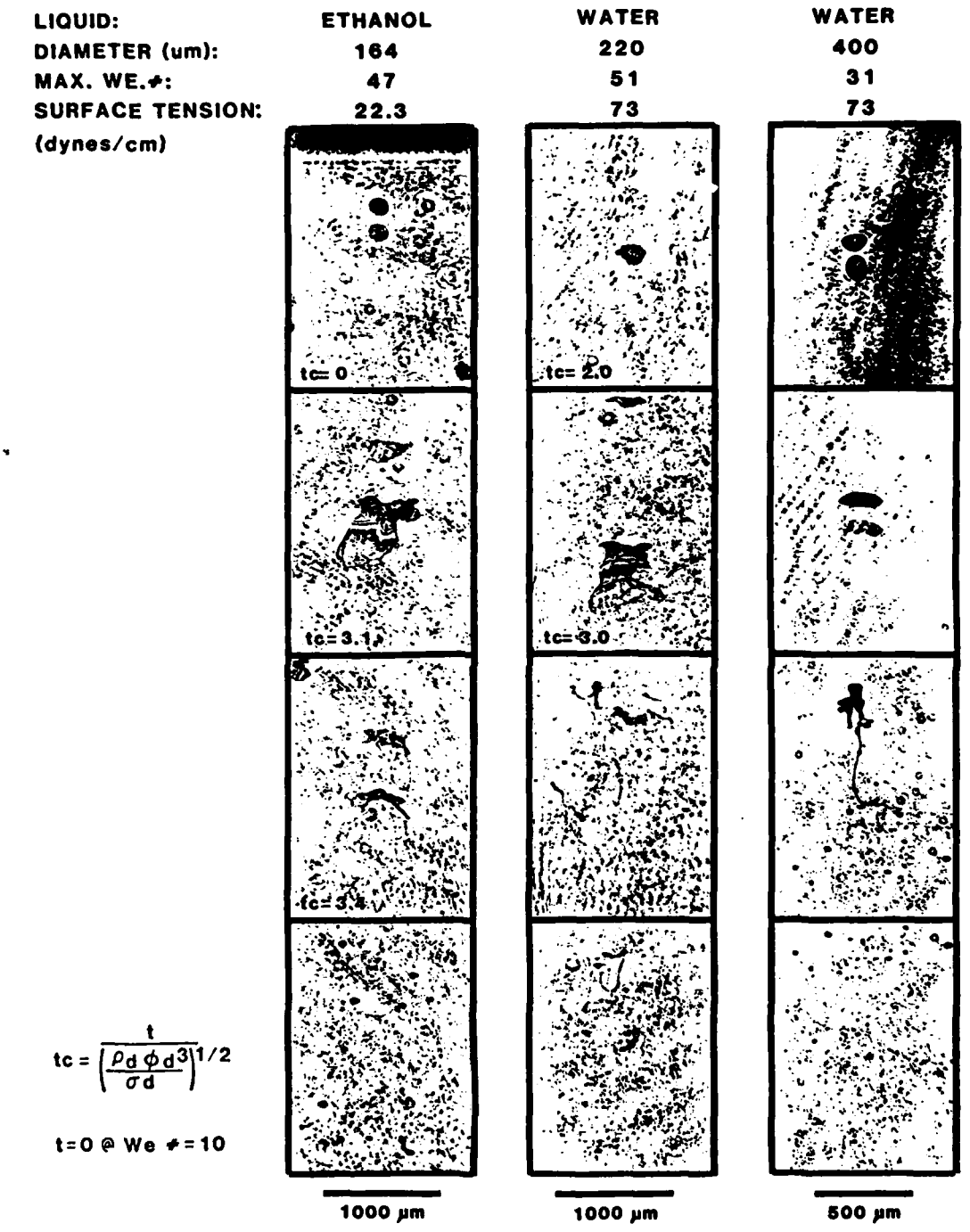

$$tc = \frac{t}{\left(\frac{\rho_d \phi_d^3}{\sigma_d}\right)^{1/2}}$$

t=0 @ We # = 10

FIGURE 4. Surface Tension Effects on Droplet Breakup

Viscous Effects

A glycerine/water mixture was used to investigate viscous effects. The mixture was selected to obtain a viscosity 10 times that of water ($\gamma_{mixture}$ = 10 cp). The significant effect of viscosity is to modify the rate of deformation in the streamwise and radial directions. Specifically, the rate of expansion in the streamwise and radial directions are observed to be about equal; and as a result, the droplets expand radially to about 7 times the original diameter (Figure 5). For the lower viscosity case, radial expansion is limited to about a factor of four or five.

The mechanism of droplet breakup is not significantly altered, however, some details are strikingly affected. For the higher viscosity case, geometric symmetry is maintained throughout substantial portions of breakup event; whereas for the lower viscosity case, the deformation quickly becomes asymmetric or random.

WEBER Number Effects

The effect of increasing the Weber number range was studied by increasing both droplet size and nozzle velocity. The factor of two increase in the peak Weber number does not appear to have changed the breakup mode. The bag is still observed to expand downstream of the ring (Figure 6). After the bag has burst, the ring exhibits more random distortion with increasing Weber number. After fragmentation is complete, the droplet size distribution is determined. Three size distributions were compiled (Figure 7). Increased Weber number is seen to decrease the size of the droplet fragments. The mean sizes and the mass weighted mean sized are plotted against Weber number (Figure 8).

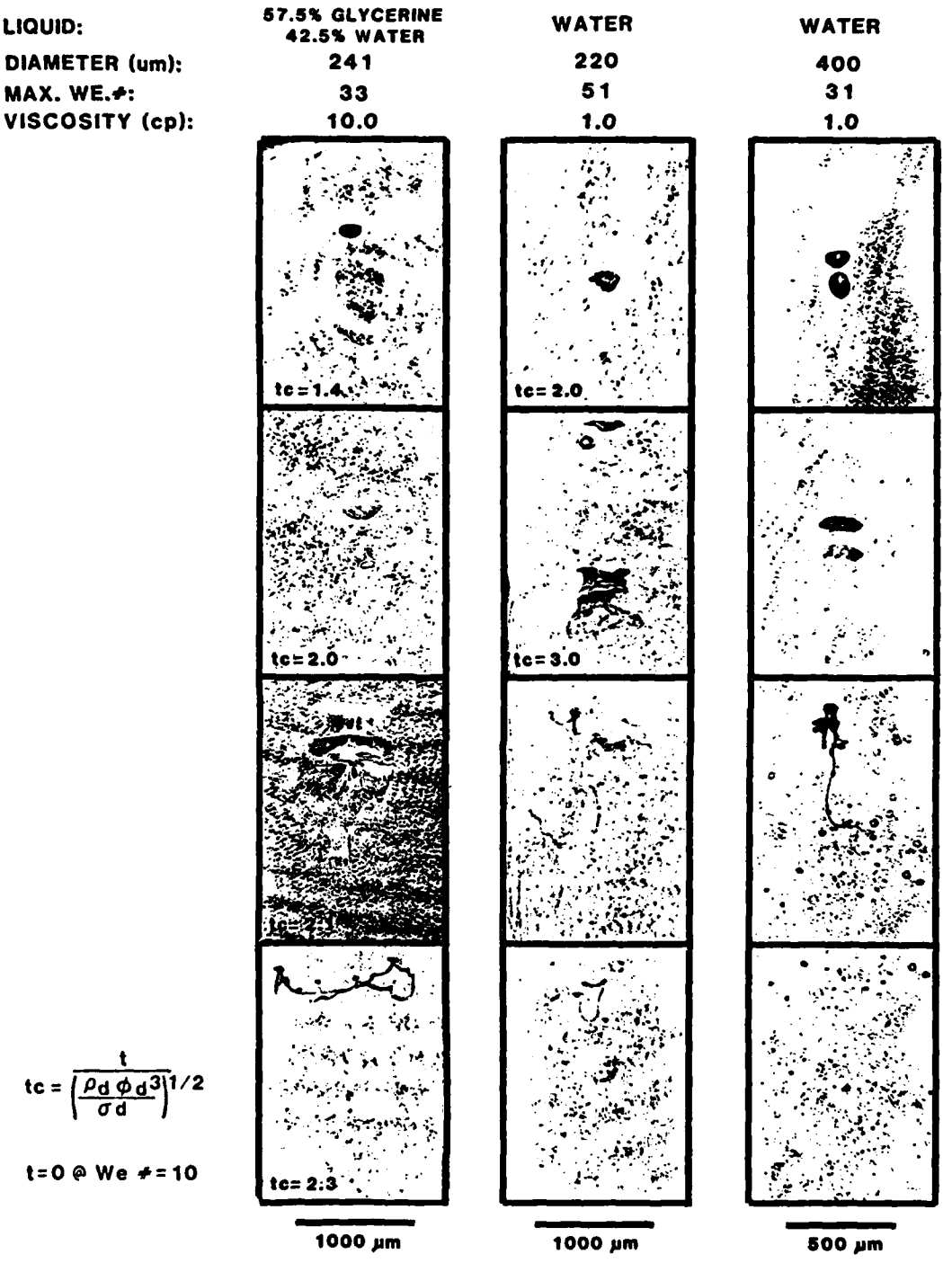

FIGURE 5. VISCOSITY EFFECTS ON DROPLET BREAKUP

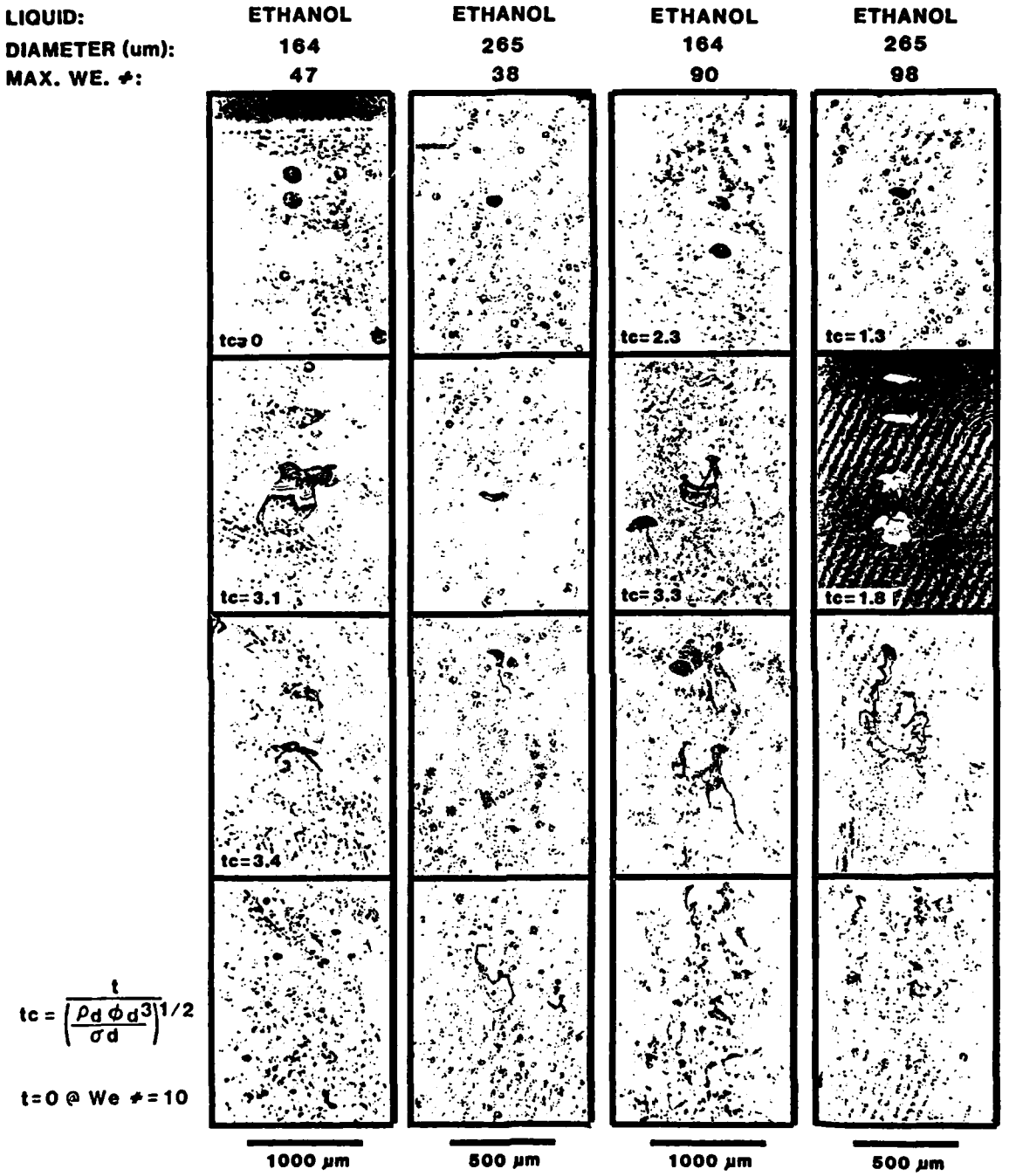

FIGURE 6. Weber Number Effects on Ethanol Droplet Breakup

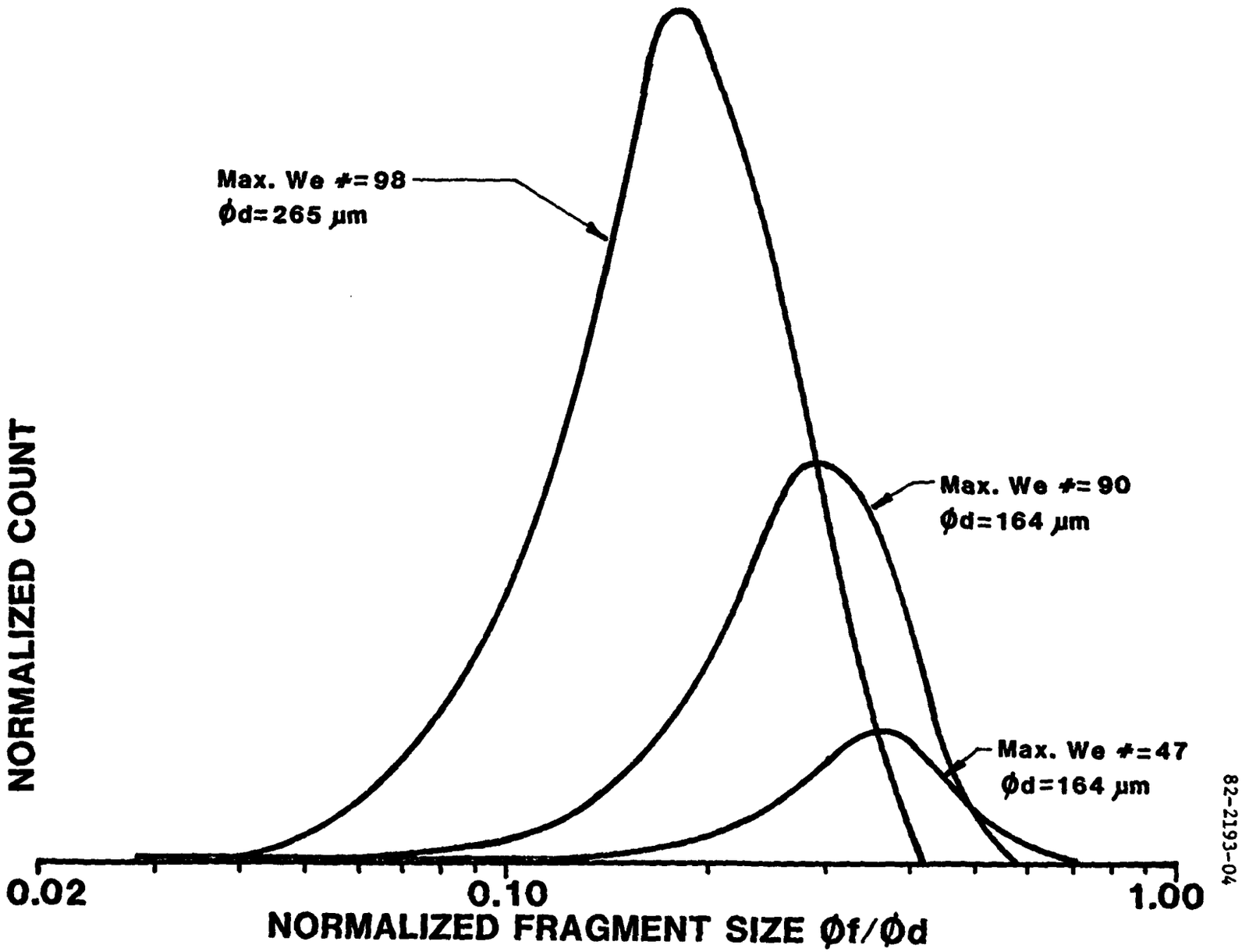

FIGURE 7. Fragment Size Distribution - Ethanol Droplets

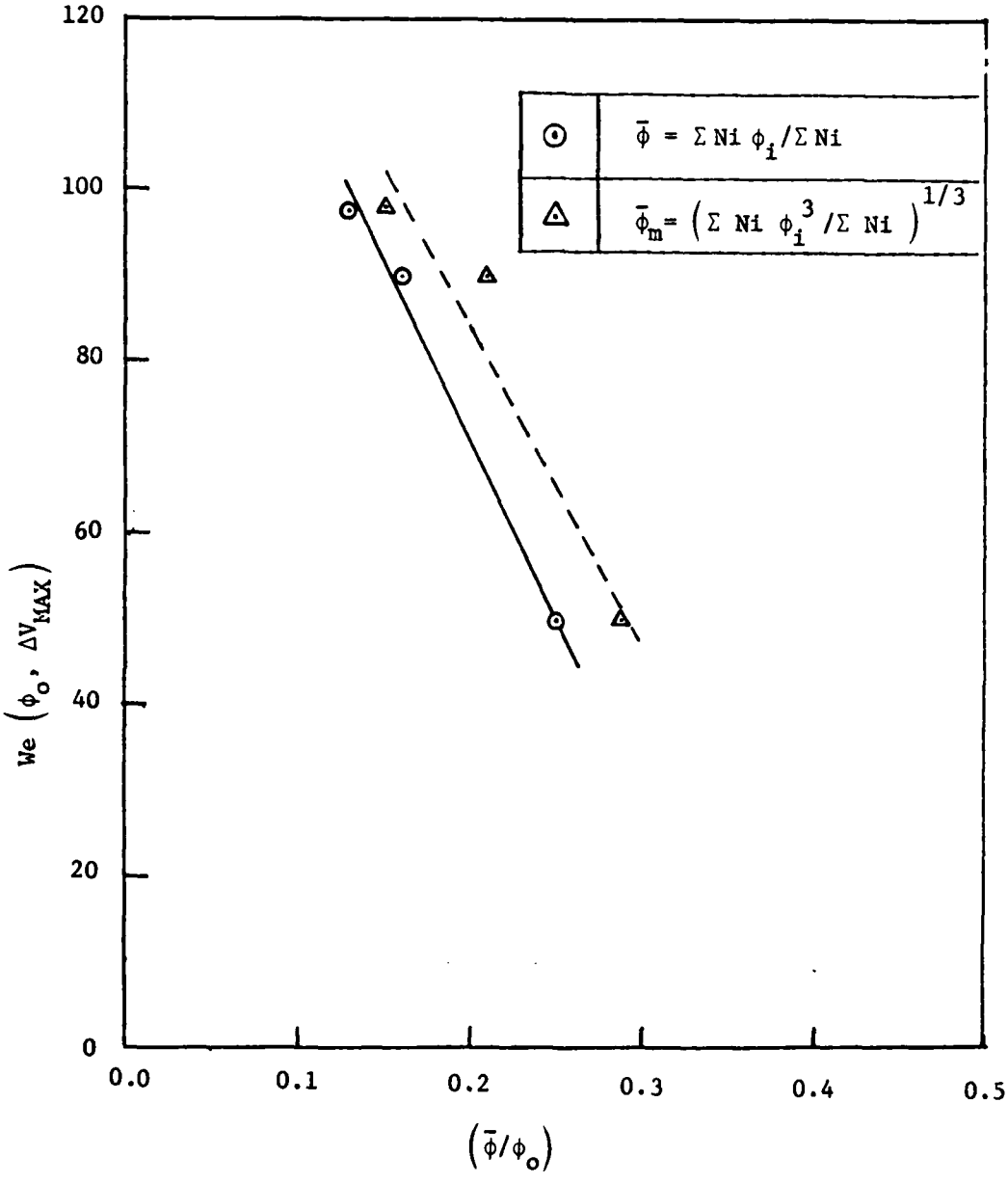

FIGURE 8. Mean Fragment Size Variation With Maximum Weber Number Based on Initial Size, ϕ_o.

Summary

A three-phase experimental investigation of the physical characterization of liquid droplet behavior within the nozzle contraction have been described. These processes are inherently dependent. Initial deformations which result in increased accelerations and decreased slip velocity affect the droplet condition at the point of fragmentation.

In the initial experiment, conventional liquids have been used to study the effects of two liquid properties, namely surface tension and viscosity. Holographic observation of the droplet acceleration, deformation and fragmentation processes within the nozzle contraction have been recorded. Holographic observations revealed the dramatic increase in droplet acceleration caused by the initial deformation. Later observations revealed classical breakup mechanisms and finally the fragment size distribution was determined.

Current and Future Efforts

The major objective of our second year's efforts will be to concentrate on the breakup dynamics of higher surface tension liquid metal droplets which more closely simulate the liquid properties of molten aluminum. Much of our current technical approach will be utilized including aerodynamic acceleration, ink jet, droplet generation, and holographic observation. The nozzle facility will be upgraded to provide the supersonic flow required to break up the higher surface tension droplets. In addition, droplet velocimetry will be attempted to accurately characterize the velocities of both the initial droplets and the resulting fragments along the nozzle. SDL has recently developed the capability to predict the motion of liquid droplets (including effects of internal circulation) in a prescribed velocity field. This

capability has significantly improved our ability to interpret experimental results and to design the liquid metal droplet experiments.

PUBLICATIONS LIST

J. E. Craig, M. Houser, "Droplet Dynamics and Fragmentation Processes in Aerodynamic Nozzle Contractions", 19th JANNAF Combustion Meeting, Greenbelt, Maryland, October 1982.

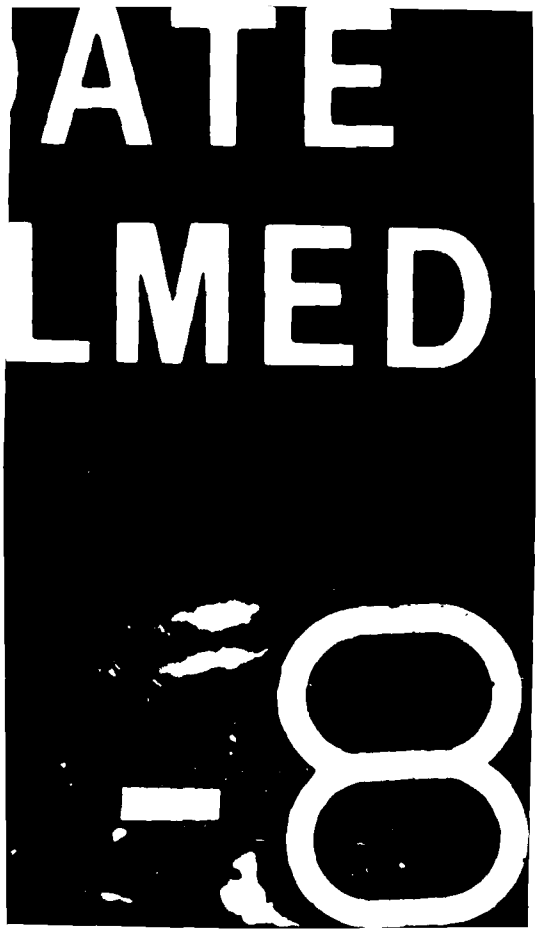
ATE
LMED
-8